

Repurpose Open Data to Discover Therapeutics for COVID-19 Using Deep Learning

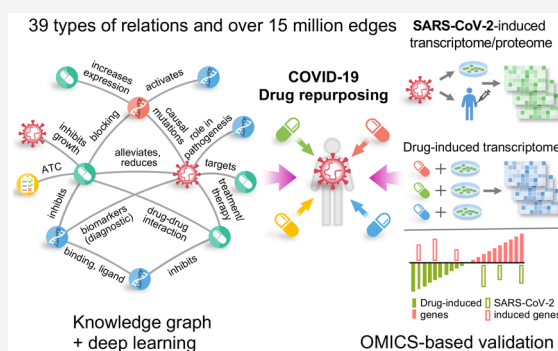
Xiangxiang Zeng,[◆] Xiang Song,[◆] Tengfei Ma,[◆] Xiaoqin Pan, Yadi Zhou, Yuan Hou, Zheng Zhang, Kenli Li, George Karypis,^{*} and Feixiong Cheng^{*} Cite This: <https://dx.doi.org/10.1021/acs.jproteome.0c00316> Read Online

ACCESS |

 Metrics & More Article Recommendations Supporting Information

ABSTRACT: There have been more than 2.2 million confirmed cases and over 120 000 deaths from the human coronavirus disease 2019 (COVID-19) pandemic, caused by the novel severe acute respiratory syndrome coronavirus (SARS-CoV-2), in the United States alone. However, there is currently a lack of proven effective medications against COVID-19. Drug repurposing offers a promising route for the development of prevention and treatment strategies for COVID-19. This study reports an integrative, network-based deep-learning methodology to identify repurposable drugs for COVID-19 (termed CoV-KGE). Specifically, we built a comprehensive knowledge graph that includes 15 million edges across 39 types of relationships connecting drugs, diseases, proteins/genes, pathways, and expression from a large scientific corpus of 24 million PubMed publications. Using Amazon's AWS computing resources and a network-based, deep-learning framework, we identified 41 repurposable drugs (including dexamethasone, indomethacin, niclosamide, and toremifene) whose therapeutic associations with COVID-19 were validated by transcriptomic and proteomics data in SARS-CoV-2-infected human cells and data from ongoing clinical trials. Whereas this study by no means recommends specific drugs, it demonstrates a powerful deep-learning methodology to prioritize existing drugs for further investigation, which holds the potential to accelerate therapeutic development for COVID-19.

KEYWORDS: COVID-19, deep learning, drug repurposing, knowledge graph, representation learning, SARS-CoV-2



INTRODUCTION

As of June 22, 2020, in the United States alone, more than 2.2 million cases and over 120 000 deaths from Coronavirus Disease 2019 (COVID-19), the disease caused by the virus SARS-CoV-2, have been confirmed.¹ However, there are currently no proven effective antiviral medications against COVID-19.² There is an urgent need for the development of effective treatment strategies for COVID-19. It was estimated that in 2015, pharmaceutical companies spent \$2.6 billion for the development of an FDA-approved new chemical entity drugs using traditional *de novo* drug discovery.³ Drug repurposing, a drug-discovery strategy using existing drugs, offers a promising route for the development of prevention and treatment strategies for COVID-19.⁴

In a randomized, controlled, open-label trial,⁵ lopinavir and ritonavir combination therapy did not show a clinical benefit compared with standard care for hospitalized adult patients with severe COVID-19, limiting the traditional antiviral treatment for COVID-19. SARS-CoV-2 replication and infection depend on the host cellular factors (including angiotensin-converting enzyme 2 (ACE2)) for entry into cells.⁶ The systematic identification of virus–host protein–protein interactions (PPIs) offers an effective way toward the

elucidation of the mechanisms of viral infection; furthermore, targeting the cellular virus–host interactome offers a promising strategy for the development of effective drug repurposing for COVID-19, as demonstrated in previous studies.^{7–9} We recently demonstrated that network-based methodologies leveraging the relationship between drug targets and diseases can serve as a useful tool for the efficient screening of potentially new indications of FDA-approved drugs with well-established pharmacokinetic/pharmacodynamic, safety, and tolerability profiles.^{10–12} Deep learning has also recently demonstrated its better performance than classic machine learning methods to assist drug repurposing,^{13–16} yet without foreknowledge of the complex networks connecting drugs, targets, SARS-CoV-2, and diseases, the development of affordable approaches for the effective treatment of COVID-19 is challenging.

Special Issue: Proteomics in Pandemic Disease

Received: May 10, 2020

Published: July 12, 2020

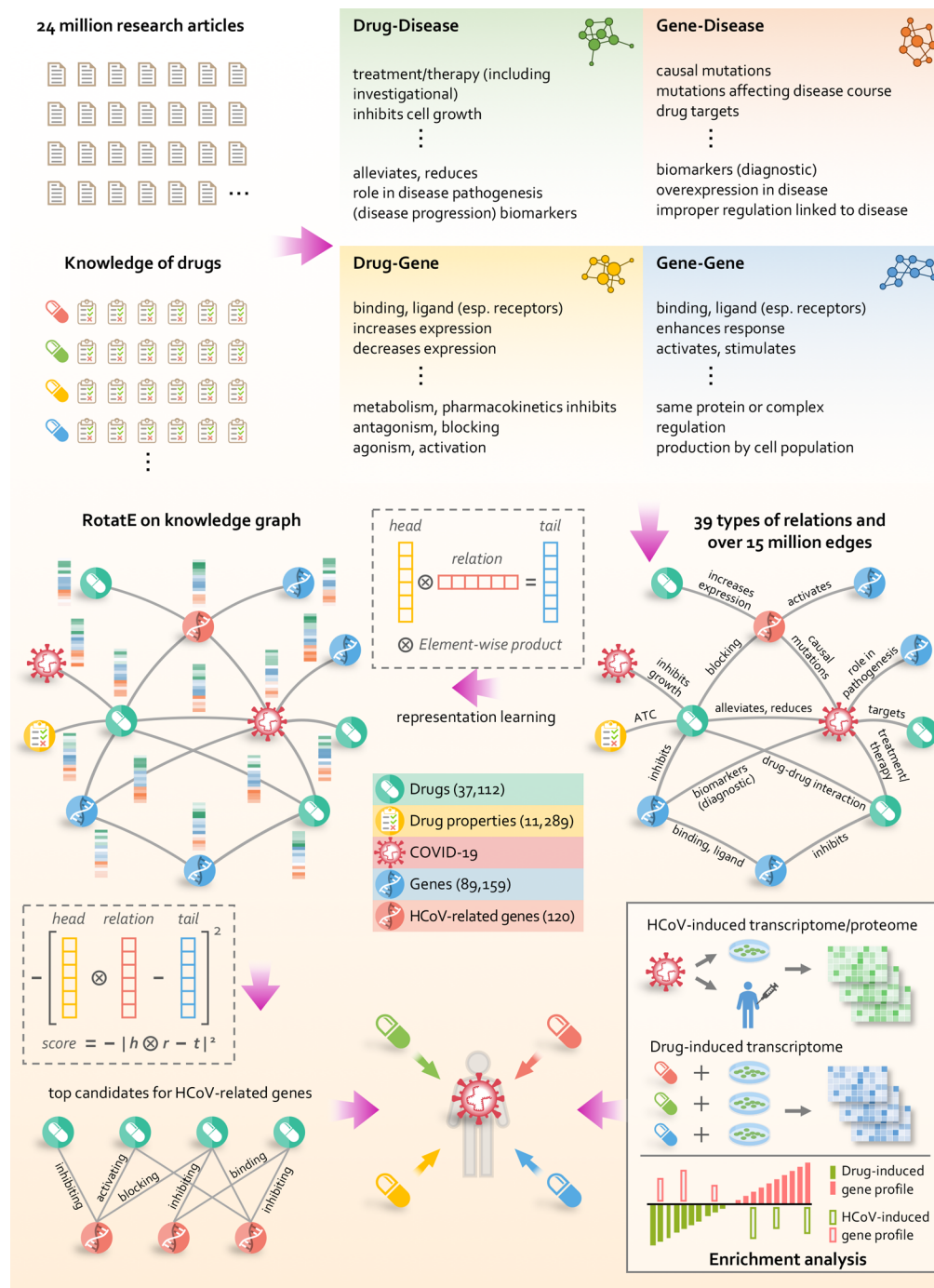


Figure 1. Diagram illustrating the workflow of a network-based, deep-learning methodology (termed CoV-KGE) for drug repurposing in COVID-19. Specifically, a comprehensive knowledge graph that contains 15 million edges across 39 types of relationships connecting drugs, diseases, genes, pathways, expressions, and others by incorporating data from 24 million PubMed publications and DrugBank (Table S2). Subsequently, a deep-learning approach (RotatE in DGL-KE) was used to prioritize high-confidence candidate drugs for COVID-19 under Amazon supercomputing resources (cf. Methods and Materials). Finally, all CoV-KGE predicted drug candidates were future-validated by three gene expression data sets in SARS-CoV-1-infected human cells and one proteomics data set in SARS-CoV-2 infected human cells.

Prior knowledge of networks from the large scientific corpus of publications offers a deep biological perspective for capturing the relationships between drugs, genes, and diseases (including COVID-19), yet extracting connections from a large-scale repository of structured medical information is challenging. In this study, we present the state-of-the-art knowledge-graph-based, deep-learning methodologies for the rapid discovery of drug candidates to treat COVID-19 from 24

million PubMed publications (Figure 1). Via systematic validation using transcriptomics and proteomics data generated from SARS-CoV-2-infected human cells and the ongoing clinical trial data, we successfully identified 41 drug candidates that can be further tested in large-scale randomized control trials for the potential treatment of COVID-19.

METHODS AND MATERIALS

Pipeline of CoV-KGE

Here we present a knowledge-graph (KG)-based, deep-learning methodology for drug repurposing in COVID-19, termed CoV-KGE (Figure 1). Our method uses DGL-KE, developed by our Amazon's AWS AI Laboratory,¹⁷ to efficiently learn embeddings of large KGs. Specifically, we construct a KG from 24 million PubMed publications¹⁸ and DrugBank,¹⁹ including 15 million edges across 39 types of relationships connecting drugs, diseases, genes, anatomies, pharmacologic classes, gene/protein expression, and others (cf. Tables S1 and S2). In this KG, we represent the Coronaviruses (CoVs) by assembling multiple types of known CoVs, including SARS-CoV-1 and MERS-CoV, as described in our recent study.⁹

We next utilized DGL-KE's knowledge graph embedding (KGE) model, RotatE,²⁰ to learn representations of the entities (e.g., drugs and targets) and relationships (e.g., inhibition relation between drugs and targets) in an informative, low-dimensional vector space. In this space, each relationship type (e.g., antagonists or agonists) is defined as a rotation from the source entity (e.g., hydroxychloroquine) to the target entity (e.g., toll-like receptor 7/9 (TLR7/9)).

Constructing the Knowledge Graph

In this study, we constructed a comprehensive KG from Global Network of Biomedical Relationships (GNBR)¹⁸ and DrugBank.¹⁹ First, from GNBR, we included in the KG relations corresponding to drug–gene interactions, gene–gene interactions, drug–disease associations, and gene–disease associations. Second, from the DrugBank database,¹⁹ we selected the drugs whose molecular mass is >230 Da and also exist in GNBR, resulting in 3481 FDA-approved and clinically investigational drugs. For these drugs, we included in the KG relationships corresponding to the drug–drug interactions and the drug side-effects, drug anatomical therapeutic chemical (ATC) codes, drug mechanisms of action, drug pharmacodynamics, and drug-toxicity associations. Third, we included the experimentally discovered CoV–gene relationships from our recent work in the KG.⁹ Fourth, we treated the COVID-19 context by assembling known genes/proteins associated with CoVs (including SARS-CoV and MERS-CoV) as a comprehensive node of CoVs and rewired the connections (edges) from genes and drugs. The resulting KG contains four types of entities (drug, gene, disease, and drug side information), 39 types of relationships (Table S1), 145 179 nodes, and 15 018 067 edges (Table S2).

Knowledge Graph Embedding Model RotatE

Models for computing KGEs learn vectors for each of the entities and each of the relation types so that they satisfy certain properties. In our work, we learned these vectors using the RotatE model.²⁰ Given an edge in the KG represented by the triplet (head entity, relation type, and tail entity), RotatE defines each relation type as a rotation from the head entity to the tail entity in the complex vector space. Specifically, if h and t are the vectors corresponding to the head and tail entities, respectively, and r is the vector corresponding to the relation type, then RotatE tries to minimize the distance

$$d_r(h, t) = \|h \otimes r - t\| \quad (1)$$

where \otimes denotes the Hadamard (element-wise) product.

To minimize the distance between the head and the tail entities of the existing triplets (positive examples) and maximize the distance among the nonexisting triplets (negative examples), we use the loss function

$$L = -\log \sigma(\gamma - d_r(h, t)) - \sum_{i=1}^n p(h_i, r, t_i) \log \sigma(d_r(h_i, t_i) - \gamma) \quad (2)$$

where σ is sigmoid function, γ is a margin hyperparameter with $\gamma > 0$, (h_i, r, t_i) is a negative triplet, and $p(h_i, r, t_i)$ is the probability of occurrence of the corresponding negative sample.

Details of DGL-KE Package

DGL-KE¹⁷ is a high-performance, easy-to-use, and scalable package for learning large-scale KGEs with a set of popular models including TransE, DistMult, ComplEx, and RotatE. It includes various optimizations that accelerate training on KGs with millions of nodes and billions of edges using multi-processing, multi-GPU (graphics processor unit), and distributed parallelism. DGL-KE is able to compute the RotatE-based embeddings of our KG in ~40 mins on an EC2 instance with 8 GPUs under Amazon's AWS computing resources.

Experimental Settings

We divide the triplets (e.g., a relationship among drug, treatment, and disease) into a training set, validation set, and test set in a 7:1:2 manner. We selected the embedding dimensionality of $\dim = 200$ for nodes and relations. The RotatE is trained for 16 000 epochs with a batch size 1024 and 0.1 as the learning rate. We choose $\gamma = 12$ as the margin of the optimization function.

Gene-Set Enrichment Analysis

Gene set enrichment analysis was performed to further validate the predicted drug candidates from CoV-KGE. The goal of the gene set enrichment analysis was to identify drugs that can reverse the cellular changes (transcriptome or proteome levels) that result from virus infection. Four differential expression data sets were collected, including two transcriptome data sets from SARS-CoV patients' peripheral blood²¹ (GSE1739) and Calu-3 cells²² (GSE33267), one transcriptome data set of Calu-3 cells infected by MERS-CoV²³ (GSE122876), and one proteome data set of human Caco-2 cells infected with SARS-CoV-2.²⁴ These four data sets were used as the gene signatures for the viral infections. For the drugs, we retrieved the Connectivity Map (CMap) database²⁵ containing the gene expression in cells treated with various drugs. An enrichment score (ES) for each CoV signature data set was calculated using a previously described method²⁶

$$ES = \begin{cases} ES_{\text{up}} - ES_{\text{down}}, & \text{sgn}(ES_{\text{up}}) \neq \text{sgn}(ES_{\text{down}}) \\ 0, & \text{else} \end{cases} \quad (3)$$

ES_{up} and ES_{down} indicate the ES values for the up- and down-regulated genes from the CoV gene signature data set. To compute $ES_{\text{up/down}}$, we first calculated $a_{\text{up/down}}$ and $b_{\text{up/down}}$ as

$$a = \max_{1 \leq j \leq s} \left(\frac{j}{s} - \frac{V(j)}{r} \right) \quad (4)$$

$$b = \max_{1 \leq j \leq s} \left(\frac{V(j)}{r} - \frac{j-1}{s} \right) \quad (5)$$

where $j = 1, 2, \dots, s$ are the genes from the CoV signature data set sorted in ascending order using the gene profiles of the drug being computed. $V(j)$ denotes the rank of j , where $1 \leq V(j) \leq r$, with r being the total number of genes (12 849) from the CMap database. Next, $ES_{\text{up/down}}$ is set to $a_{\text{up/down}}$ if $a_{\text{up/down}} > b_{\text{up/down}}$ and is set to $-b_{\text{up/down}}$ if $b_{\text{up/down}} > a_{\text{up/down}}$. Permutation tests are repeated 100 times to quantify the significance of the ES score. In each repeat, the same number of up- and down- expressed genes as the CoV signature data set was randomly generated. $ES > 0$ and $P < 0.05$ are considered significantly enriched. The number of significantly enriched data sets is used as the final result for a certain drug.

Performance Evaluation

We introduced the area under the receiver operating characteristic (ROC) curve (AUROC) and several evaluation metrics for evaluating the performance of drug–target interaction prediction. The AUROC²⁷ is the global prediction performance. The ROC curve is obtained by calculating the true-positive rate (TPR) and the false-positive rate (FPR) via varying cutoffs.

RESULTS

High Performance of CoV-KGE

After mapping drugs, CoVs, and the treatment relationships to a complex vector space using RotatE, the top 100 most relevant drugs were selected as candidates for CoVs in the treatment relation space (Figure S1). Using the ongoing COVID-19 trial data (<https://covid19-trials.com/>) as a validation set, CoV-KGE has a larger AUROC (AUROC = 0.85, Figure 2) for identifying repurposable drugs for COVID-19.

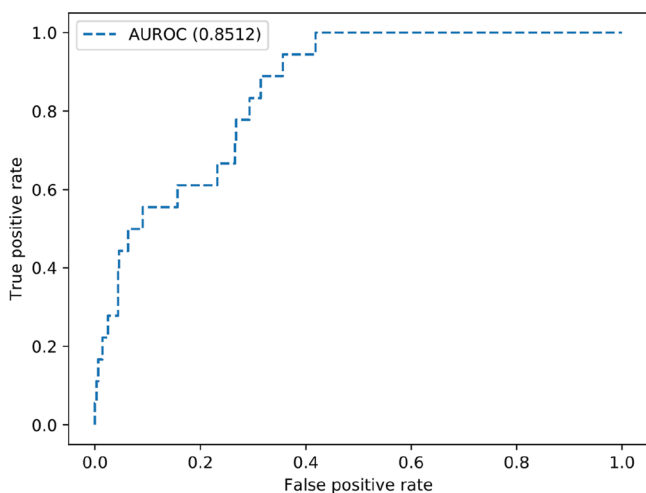


Figure 2. Performance of CoV-KGE in the prediction of drug candidates for COVID-19. Drugs in the ongoing COVID-19 trial data (<https://covid19-trials.com/>) were used as the validation set. AUROC, area under the ROC curve.

We next employ t-SNE (t-distributed stochastic neighbor embedding algorithm²⁸) to further investigate the low-dimensional node representation learned by CoV-KGE. Specifically, we projected drugs grouped by the first level of the Anatomical Therapeutic Chemical (ATC) classification systems code onto a 2D space. Figure 3A indicates that CoV-KGE is able to distinguish 14 types of drugs grouped by ATC

codes, which is consistent with a high AUROC value of 0.85 (Figure 2).

We further validated the top candidate drugs using an enrichment analysis of drug–gene signatures and SARS-CoV-induced transcriptomics and proteomics data in human cell lines (cf. Methods and Materials). Specifically, we analyzed three transcriptomic data sets in SARS-CoV-1-infected human cell lines and one proteomics data set in SARS-CoV-2-infected human cell lines. In total, we obtained 41 repositioned drug candidates (Table 1) using subject-matter expertise based on a combination of factors: (i) the strength of the CoV-KGE predicted score, (ii) the availability of clinical evidence from ongoing COVID-19 trials, and (iii) the availability and strength of enrichment analyses from SARS-CoV-1/2-affected human cell lines. Among the 41 candidate drugs, 9 drugs are or have been under clinical trials for COVID-19, including thalidomide, methylprednisolone, ribavirin, umifenovir, tetrandrine, suramin, dexamethasone, lopinavir, and azithromycin (Figure 3A and Table 1). We excluded chloroquine and hydroxychloroquine from our ongoing clinical trial list based on recently controversial reports.^{29,30}

Discovery of Drug Candidates for COVID-19 Using CoV-KGE

We next turned to highlight three types of predicted drugs for COVID-19, including anti-inflammatory agents (dexamethasone, indomethacin, and melatonin), selective estrogen receptor modulators (SERMs), and antiparasitics (Figure 3).

Anti-Inflammatory Agents. Given the well-described lung pathophysiological characteristics and immune responses (cytokine storms) of severe COVID-19 patients, drugs that dampen the immune responses may offer effective treatment approaches for COVID-19.^{31,32} As shown in Figure 3A, we computationally identified multiple anti-inflammatory agents for COVID-19, including dexamethasone, indomethacin, and melatonin. Indomethacin, an approved cyclooxygenase (COX) inhibitor, has been widely used for its potent anti-inflammatory and analgesic properties.³³ Indomethacin has been reported to have antiviral properties, including SARS-CoV-1³³ and SARS-CoV-2.³⁴ Importantly, a preliminary *in vivo* observation showed that oral indomethacin (1 mg/kg body weight daily) reduced the recovery time of SARS-CoV-2-infected dogs.³⁴ Melatonin plays a key role in the regulation of the human circadian rhythm that alters the translation of thousands of genes, including melatonin-mediated anti-inflammatory and immune-related effects for COVID-19. Melatonin has various antiviral activities by suppressing multiple inflammatory pathways^{35,36} (i.e., IL6 and IL-1 β); these inflammatory effects are directly relevant given the well-described lung pathophysiological characteristics of severe COVID-19 patients. Melatonin's mechanism of action may also help to explain the epidemiologic observation that children, who have naturally high melatonin levels, are relatively resistant to COVID-19 disease manifestations, whereas older individuals, who have decreasing melatonin levels with age, are a very high-risk population.³⁷ In addition, exogenous melatonin administration may be of particular benefit to older patients given the aging-related reduction of endogenous melatonin levels and the vulnerability of older individuals to the lethality of SARS-CoV-2.³⁷

Dexamethasone is a U.S. FDA-approved glucocorticoid receptor (GR) agonist for a variety of inflammatory and autoimmune conditions, including rheumatoid arthritis, severe

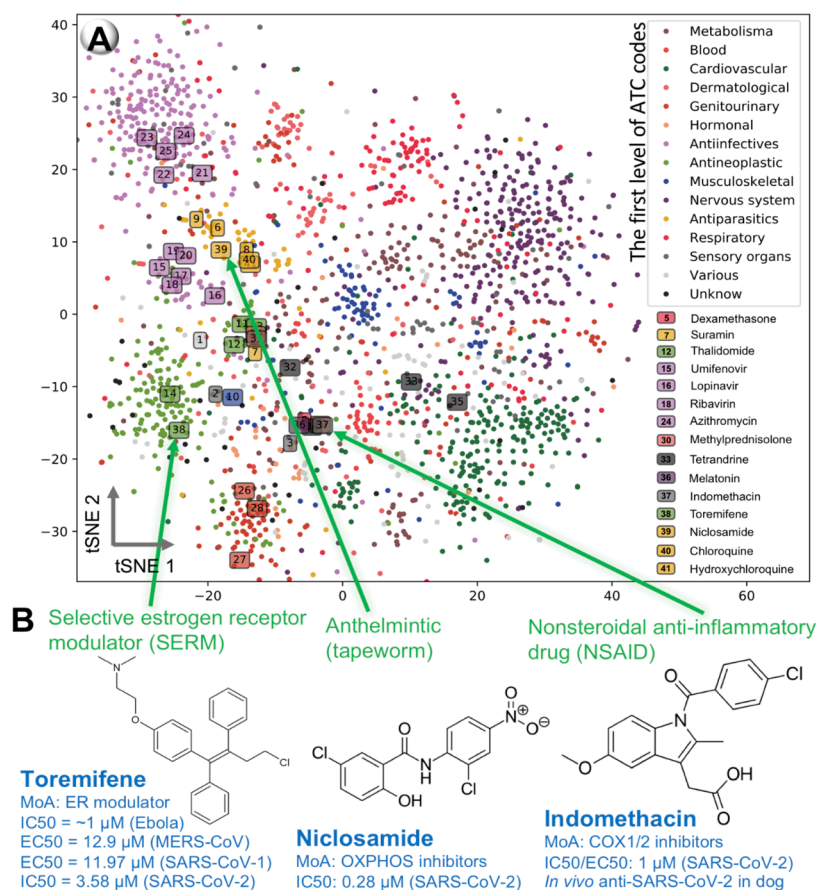


Figure 3. Diagram illustrating the landscape of CoV-KGE-predicted repurposable drugs for COVID-19. (A) Visualization of the drug vector learned by the knowledge graph embedding using t-SNE (t-distributed stochastic neighbor embedding algorithm²⁸). 2D representation of the learned vectors for 14 types of drugs grouped by the first level of the Anatomical Therapeutic Chemical (ATC) classification system codes. Semantically similar ATC drugs are mapped to nearby representations. We highlighted 11 drugs that are under clinical trials for COVID-19. (B) Three highlighted drugs (toremifene, niclosamide, and indomethacin) having striking *in vitro* antiviral activities across Ebola virus,^{42,43} MERS-CoV,⁴⁴ SARS-CoV-1,⁴⁵ and SARS-CoV-2.⁴⁶

allergies, asthma, chronic obstructive lung disease, and others.³⁸ Glucocorticoid medications have been used in patients with MERS-CoV and SARS-CoV-1 infections.³⁹ As shown in Figure 3A, dexamethasone is the fourth predicted drug among 41 candidates. The Randomized Evaluation of COVID-19 therapy (RECOVERY, [ClinicalTrials.gov](https://clinicaltrials.gov/ct2/show/study/NCT04381936) Identifier: NCT04381936) trial showed that dexamethasone reduced mortality by one-third in patients requiring ventilation and by one-fifth in individuals requiring oxygen,⁴⁰ yet dexamethasone did not reduce death in COVID-19 patients not receiving respiratory support.⁴⁰

Selective Estrogen Receptor Modulators. An over-expression of the estrogen receptor has played a crucial role in inhibiting viral replication and infection.⁴¹ Several SERMs, including clomifene, bazedoxifene, and toremifene, are identified as promising candidate drugs for COVID-19 (Figure 3A and Table 1). Toremifene, the first generation of the nonsteroidal SERM, was reported to block various viral infections at low micromolar concentration, including Ebola virus,^{42,43} MERS-CoV,⁴⁴ SARS-CoV-1,⁴⁵ and SARS-CoV-2⁴⁶ (Figure 3B). Toremifene prevents fusion between the viral and endosomal membranes by interacting with and destabilizing the virus glycoprotein and eventually blocking replications of the Ebola virus.⁴² The underlying antiviral mechanisms of SARS-CoV-1 and SARS-CoV-2 for toremifene remain unclear

and are currently being investigated. Toremifene has been approved for the treatment of advanced breast cancer⁴⁷ and has also been studied in men with prostate cancer (~1500 subjects) with reasonable tolerability.⁴⁸ Toremifene is 99% bound to plasma protein with good bioavailability and typically orally administered at a dosage of 60 mg.⁴⁹ In summary, toremifene is a promising candidate drug with ideal pharmacokinetics properties to be directly tested in COVID-19 clinical trials.

Antiparasitics. Despite the lack of strong clinical evidence, hydroxychloroquine and chloroquine phosphate, two approved antimalarial drugs, were authorized by the U.S. FDA for the treatment of COVID-19 patients using emergency use authorizations (EUAs).² In this study, we identified that both hydroxychloroquine and chloroquine are among the predicted candidates for COVID-19 (Figure 3A and Table 1). Between the two, hydroxychloroquine's *in vitro* antiviral activity against SARS-CoV-2 is stronger than that of chloroquine (hydroxychloroquine: 50% effective concentration (EC_{50}) = 6.14 μ M, whereas for chloroquine: EC_{50} = 23.90 μ M).⁵⁰ Hydroxychloroquine and chloroquine are known to increase the pH of endosomes, which inhibits membrane fusion, a required mechanism for viral entry (including SARS-CoV-2) into the cell.¹⁹ Although chloroquine and hydroxychloroquine are relatively well tolerated, several adverse effects

Table 1. Lists of the Selected 41 Top Drugs with the Potential to Treat COVID-19^a

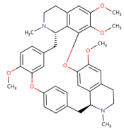
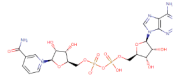
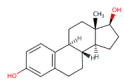
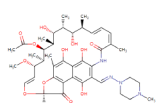
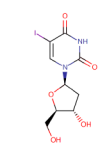
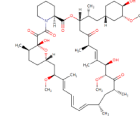
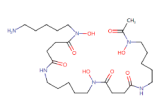
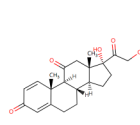
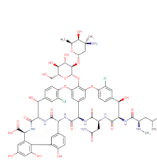
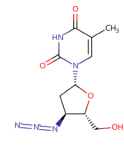
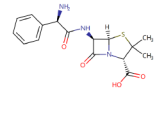
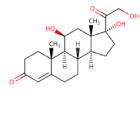
| Drug Name | Enrichment analysis | Structure | Category | PubMed or Clinic trial id |
|----------------|---------------------|---|-----------------------------------|--|
| Tetrandrine* | 3 |  | Adenine Nucleotides | <u>NCT04308317</u> |
| Nadide | 4 |  | Adenine Nucleotides | 27134728 |
| Estradiol | 4 |  | Adrenal Cortex Hormones | 28373583 32052466 32199468 |
| Rifampicin | 3 |  | Anti-Bacterial Agents | 15227635 10517189 28683463 |
| Idoxuridine | 4 |  | Anti-Infective Agents | 31216912 30937274 |
| Sirolimus | 4 |  | Anti-Bacterial Agents | 29143192 25487801 32194980 32161092 |
| Deferoxamine | 3 |  | Chelating Agents | 6954069 24323450 25535360 16542729 |
| Prednisone | 3 |  | Adrenal Cortex Hormones | 16968120 32043983 29143192 16675038 |
| Vancomycin | 3 |  | Anti-Bacterial Agents | 12877785 25828287 26953343 29143192 |
| Zidovudine | 3 |  | Anti-HIV Agents | 31925415 29161116 15200845 |
| Ampicillin | 3 |  | Anti-Bacterial Agents | 28148787 15356814 23978488 29227752 |
| Hydrocortisone | 3 |  | 11- Hydroxycorticoste roids | 27585965 15647850 15494274 |

Table 1. continued

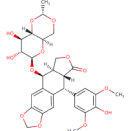
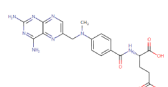
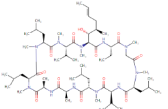
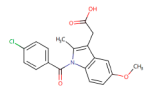
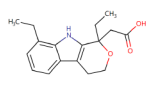
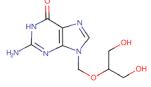
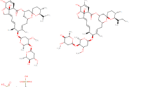
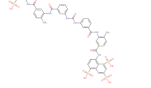
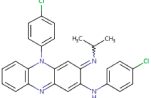
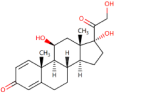
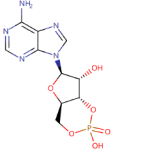
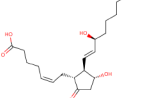
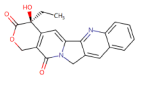
| Drug Name | Enrichment analysis | Structure | Category | PubMed or Clinic trial id |
|--------------------------------|---------------------|---|-----------------------------|--|
| Etoposide | 3 |  | Antineoplastic Agents | 28817732 26365771 32194944 32113509 |
| Methotrexate | 3 |  | Abortifacient Agents | 2805607 29496347 25084201 29772254 |
| Cyclosporine | 3 |  | Agents causing hyperkalemia | 23620378 27097824 23396219 17302372 |
| Indomethacin | 3 |  | Analgesics | 25856684 24096239 17555580 30581611 |
| Etodolac | 2 |  | Agents causing hyperkalemia | 32105468 30206897 32023685 |
| Ganciclovir | 2 |  | Anti-Infective Agents | 15200845 32169119 32251768 24841269 |
| Ivermectin | 2 |  | Agrochemicals | 32251768 24841269 |
| Suramin* | 2 |  | Acids | <u>CHICTR2000030016</u> |
| Clofazimine | 2 |  | Anti-Infective Agents | 30202770 |
| Prednisolone | 2 |  | Adrenal Cortex Hormones | 16542729 29143192 16968120 |
| Cyclic adenosine monophosphate | 2 |  | Adenine Nucleotides | 24453361 |
| Dinoprostone | 2 |  | Biological Factors | 30315411 11878905 |
| Camptothecin | 2 |  | Antineoplastic Agents | |

Table 1. continued

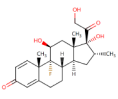
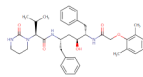
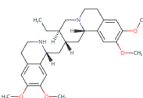
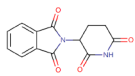
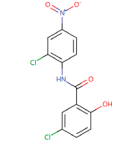
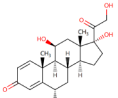
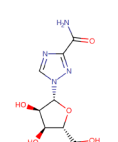
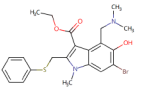
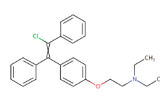
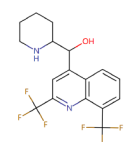
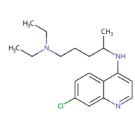
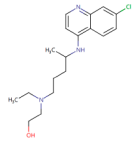
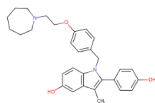
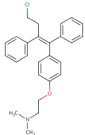
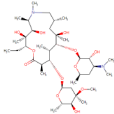
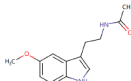
| Drug Name | Enrichment analysis | Structure | Category | PubMed or Clinic trial id |
|---------------------|---------------------|---|--------------------------------|--|
| Dexamethasone* | 2 |  | Adrenal Cortex Hormones | NCT04325061 |
| Lopinavir* | 2 |  | Anti-Infective Agents | CHICTR2000029468 32251767 |
| Emetine | 1 |  | Agents Causing Muscle Toxicity | 29143192 32245264 30918074 |
| Thalidomide* | 1 |  | Acids, Carbocyclic | NCT04273529 |
| Nicosamide | 1 |  | Agrochemicals | 15215127 32125140 31852899 |
| Methylprednisolone* | 1 |  | Adrenal Cortex Hormones | NCT04323592 |
| Ribavirin* | 1 |  | Anti-Infective Agents | CHICTR2000030922 |
| Umifenovir* | 1 |  | Antiviral Agents | NCT04252885 |
| Clomifene | 1 |  | Clomiphene | 25256397 30284220 19821295 |
| Mefloquine | 1 |  | Anti-Infective Agents | 32149769 29143192 32127666 |
| Chloroquine | 0 |  | Agents Causing Muscle Toxicity | 32194981 |
| Hydroxychloroquine | 0 |  | Anti-Infective Agents | 32194981 |

Table 1. continued

| Drug Name | Enrichment analysis | Structure | Category | PubMed or Clinic trial id |
|---------------|---------------------|---|----------------------------------|----------------------------------|
| Bazedoxifene | 0 |  | Bone Density Conservation Agents | 30852762 31587108 |
| Toremifene | 0 |  | Anti-Estrogens | 24841273 29143192 32194980 |
| Azithromycin* | 0 |  | Anti-Bacterial Agents | <u>NCT04332107</u> |
| Melatonin | - |  | Antioxidants | 32217117 32194980 29769094 |

^aNote: Drugs marked with * are in clinical trials. All predicted drugs are freely available at <https://github.com/ChengF-Lab/CoV-KGE>. Enrichment scores (ESs) indicate the number of significantly enriched data sets for the drug.

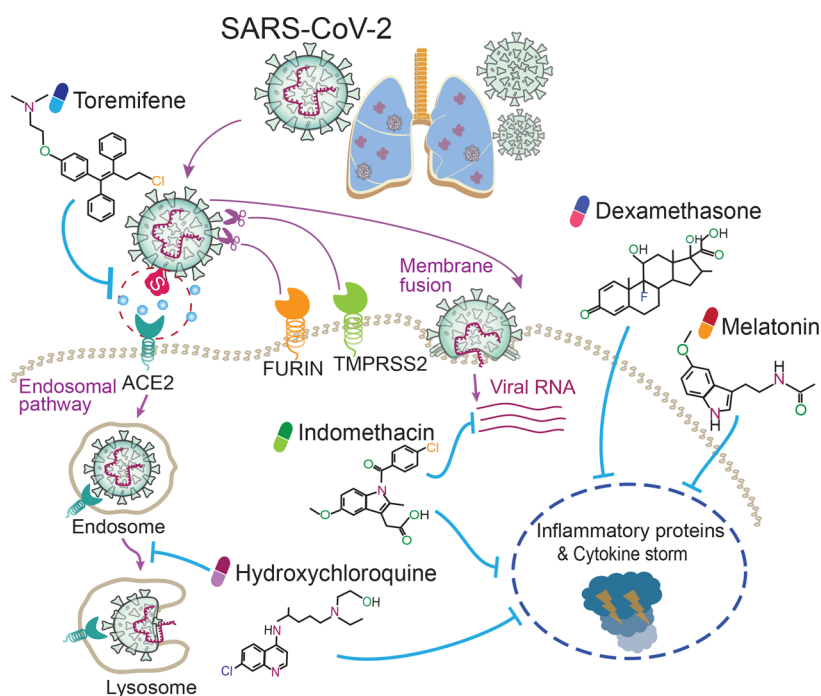


Figure 4. Proposed mechanism-of-action model that combines antiviral and anti-inflammatory agents for the potential treatment of COVID-19. Toremifene, a selective estrogen receptor modulator approved by the U.S. FDA for the treatment of advanced breast cancer, has shown various antiviral activities across Ebola virus,^{42,43} MRES-CoV,⁴⁴ SARS-CoV-1,⁴⁵ and SARS-CoV-2.⁴⁶ Melatonin is a synthesized hormone with ~2.5 billion years history. Given the well-described lung injury characteristics of severe COVID-19 by multiple inflammatory pathways,^{35,36} dexamethasone, indomethacin, and melatonin are candidate anti-inflammatory agents for the treatment of patients with COVID-19 (Figure 3A). Thus combining antiviral (toremifene or hydroxychloroquine) and anti-inflammatory agents (dexamethasone, indomethacin, or melatonin) may provide an effective treatment for COVID-19, as demonstrated in ongoing COVID-19 trials (remdesivir plus baricitinib, [clinicalTrials.gov Identifier: NCT04373044](https://clinicaltrials.gov/ct2/show/study/NCT04373044)). ACE2, Angiotensin-converting enzyme 2; TMPRSS2, Transmembrane Serine Protease 2.

(including QT prolongation) limit their clinical use for COVID-19 patients, especially for patients with pre-existing cardiovascular disease or diabetes.^{10,51–53} A recent observational study reported that hydroxychloroquine administration was not associated with either a greatly lowered or an increased risk of the composite end point of intubation or death for

patients with COVID-19 who had been admitted to the hospital.³⁵ As June 15, 2020, the U.S. FDA revoked the EUAs for hydroxychloroquine and chloroquine for the treatment of COVID-19 patients.²⁹ As June 20, 2020, the National Institutes of Health halted the clinical trial of hydroxychloroquine owing to the lack of clinical benefits.³⁰ Thus further

functional observations are urgently needed to investigate the inconsistent results between *in vitro* antiviral activities and clinical efficiency in the near future.

Niclosamide, an FDA-approved drug for the treatment of tapeworm infestation, was recently identified to have a stronger inhibitory activity on SARS-CoV-2 at the submicromolar level ($IC_{50} = 0.28 \mu M$). Gassen et al. showed that niclosamide inhibited SKP2 activity by enhancing autophagy and reducing MERS-CoV replication as well.⁵⁴ Altogether, niclosamide may be another drug candidate for COVID-19, which is warranted to be investigated experimentally and further tested in randomized controlled trials.

Given the up-regulation of systemic inflammation—in some cases, culminating to a cytokine storm observed in severe COVID-19 patients³¹—combination therapy with an agent targeting inflammation (melatonin, dexamethasone, or indomethacin) and with direct antiviral effects (toremifene and niclosamide) has the potential to lead to successful treatments (Figure 4). Because of the aging-related reduction of endogenous melatonin levels and the vulnerability of older individuals to the lethality of SARS-CoV-2,³⁷ combining exogenous melatonin administration and antiviral agents (such as toremifene or niclosamide) may be of particular benefit to older patients with COVID-19. Yet all computationally predicted drug candidates (Table 1) and proposed drug combinations (Figure 4) must be validated experimentally and be tested in randomized controlled trials. Several combination antiviral and anti-inflammatory treatment trials (remdesivir plus baricitinib) are underway for patients with COVID-19 (clinicalTrials.gov Identifier: NCT04373044), indicating the proof-of-concept of this combination therapy for COVID-19.

DISCUSSION

As COVID-19 patients flood hospitals worldwide, physicians are trying to search for effective antiviral therapies to save lives. Multiple COVID-19 vaccine trials are underway, yet it might not be physically possible to make enough vaccines for everyone in a short period of time. Furthermore, SARS-CoV-2 replicates poorly in multiple animals, including dogs, pigs, chickens, and ducks, which limits preclinical animal studies.⁵⁵

To fight the emerging COVID-19 pandemic, we introduced an integrative, network-based, deep-learning methodology to discover candidate drugs for COVID-19, named CoV-KGE. Via CoV-KGE, we built a comprehensive KG that includes 15 million edges across 39 types of relationships connecting drugs, diseases, proteins/genes, pathways, and expressions from a large scientific corpus of 24 million PubMed publications. Using the ongoing COVID-19 trial data as a validation set, we demonstrated that CoV-KGE had high performance in identifying repurposable drugs for COVID-19, indicated by the larger AUROC (AUROC = 0.85). Using Amazon's AWS computing resources, we identified 41 high-confidence repurposed drug candidates (including dexamethasone, indomethacin, niclosamide, and toremifene) for COVID-19, which were validated by an enrichment analysis of gene expression and proteomics data in SARS-CoV-2 infected human cells. Altogether, this study offers a powerful, integrated deep-learning methodology for the rapid identification of repurposable drugs for the potential treatment of COVID-19.

We acknowledge several potential limitations in the current study. Potential data noises generated from different experimental approaches in large-scale publications may

influence the performance of the current CoV-KGE models. The original data of GNBR contain the confidence values of the relations between entities. However, we ignored the weights so that we could directly apply the RotatE algorithm because we tried to obtain the prediction result in a cheap computing-cost way. In our future work, we will take these confidence values into account and try to design a knowledge-graph-embedding algorithm that can be used for a KG with weighted relationships. The lack of dose-dependent profiles and the biological perturbation of SARS-CoV-2 virus–host interactions may generate a coupled interplay between adverse and therapeutic effects. The integration of pharmacokinetics data from animal models and clinical trials into our CoV-KGE methodology could establish the causal mechanism and patient evidence through which predicted drugs would have high clinical benefits for COVID-19 patients without obvious adverse effects in a specific dosage.

In summary, we presented CoV-KGE, a powerful, integrated AI methodology that can be used to quickly identify drugs that can be repurposed for the potential treatment of COVID-19. Our approach can minimize the translational gap between preclinical testing results and clinical outcomes, which is a significant problem in the rapid development of efficient treatment strategies for the COVID-19 pandemic. From a translational perspective, if broadly applied, the network tools developed here could help develop effective treatment strategies for other emerging infectious diseases and other emerging complex diseases as well. However, all predicted drugs not used in clinical trials must be tested in randomized clinical trials before being used in COVID-19 patients.

ASSOCIATED CONTENT

Supporting Information

The Supporting Information is available free of charge at <https://pubs.acs.org/doi/10.1021/acs.jproteome.0c00316>.

Supplementary Figure 1. Diagram illustrating the prioritization of drugs based on their distance to COVID-19 in the treatment relation space. Supplementary Table 1. Details of the five categories of relationships in our KG. Supplementary Table 2. Statistics of nodes (entity) and edges (relation) in our KG (PDF)

AUTHOR INFORMATION

Corresponding Authors

George Karypis – AWS AI, East Palo Alto, California 94303, United States; Department of Computer Science and Engineering, University of Minnesota, Minneapolis, Minnesota 55455, United States; Email: karypis@umn.edu

Feixiong Cheng – Genomic Medicine Institute, Lerner Research Institute, Cleveland Clinic, Cleveland, Ohio 44106, United States; Department of Molecular Medicine, Cleveland Clinic Lerner College of Medicine, Case Western Reserve University, Cleveland, Ohio 44195, United States; Case Comprehensive Cancer Center, Case Western Reserve University School of Medicine, Cleveland, Ohio 44106, United States; orcid.org/0000-0002-1736-2847; Email: chengf@ccf.org

Authors

Xiangxiang Zeng – School of Computer Science and Engineering, Hunan University, Changsha 410012, China

Xiang Song – AWS Shanghai AI Lab, Shanghai 200335, China

Tengfei Ma – School of Computer Science and Engineering, Hunan University, Changsha 410012, China

Xiaoqin Pan – School of Computer Science and Engineering, Hunan University, Changsha 410012, China

Yadi Zhou – Genomic Medicine Institute, Lerner Research Institute, Cleveland Clinic, Cleveland, Ohio 44106, United States

Yuan Hou – Genomic Medicine Institute, Lerner Research Institute, Cleveland Clinic, Cleveland, Ohio 44106, United States

Zheng Zhang – AWS Shanghai AI Lab, Shanghai 200335, China; New York University Shanghai, Shanghai 200122, China

Kenli Li – School of Computer Science and Engineering, Hunan University, Changsha 410012, China

Complete contact information is available at:

<https://pubs.acs.org/10.1021/acs.jproteome.0c00316>

Author Contributions

◆X.Z., X.S., and T.M. are joint first authors on this work.

Notes

The authors declare no competing financial interest.

Source code and data can be downloaded from <https://github.com/ChengF-Lab/CoV-KGE>.

ACKNOWLEDGMENTS

We acknowledge support from the Amazon Cloud, for credits to AWS ML Services. The therapeutics discussed in this study are computationally predicted and are not currently approved for the treatment of COVID-19. The content of this publication does not necessarily reflect the views of the Cleveland Clinic.

REFERENCES

- (1) Dong, E.; Du, H.; Gardner, L. An interactive web-based dashboard to track COVID-19 in real time. *Lancet Infect. Dis.* **2020**, *20*, 533–534.
- (2) Sanders, J. M.; Monogue, M. L.; Jodlowski, T. Z.; Cutrell, J. B. Pharmacologic treatments for Coronavirus disease 2019 (COVID-19): A Review. *JAMA* **2020**, *323* (18), 1824–1836.
- (3) Avorn, J. The \$2.6 billion pill–methodologic and policy considerations. *N. Engl. J. Med.* **2015**, *372* (20), 1877–9.
- (4) Harrison, C. Coronavirus puts drug repurposing on the fast track. *Nat. Biotechnol.* **2020**, *38* (4), 379–381.
- (5) Cao, B.; Wang, Y.; Wen, D.; Liu, W.; Wang, J.; Fan, G.; Ruan, L.; Song, B.; Cai, Y.; Wei, M.; Li, X.; Xia, J.; Chen, N.; Xiang, J.; Yu, T.; Bai, T.; Xie, X.; Zhang, L.; Li, C.; Yuan, Y.; Chen, H.; Li, H.; Huang, H.; Tu, S.; Gong, F.; Liu, Y.; Wei, Y.; Dong, C.; Zhou, F.; Gu, X.; Xu, J.; Liu, Z.; Zhang, Y.; Li, H.; Shang, L.; Wang, K.; Li, K.; Zhou, X.; Dong, X.; Qu, Z.; Lu, S.; Hu, X.; Ruan, S.; Luo, S.; Wu, J.; Peng, L.; Cheng, F.; Pan, L.; Zou, J.; Jia, C.; Wang, J.; Liu, X.; Wang, S.; Wu, X.; Ge, Q.; He, J.; Zhan, H.; Qiu, F.; Guo, L.; Huang, C.; Jaki, T.; Hayden, F. G.; Horby, P. W.; Zhang, D.; Wang, C. A trial of lopinavir-ritonavir in adults hospitalized with severe COVID-19. *N. Engl. J. Med.* **2020**, *382* (19), 1787–1799.
- (6) Hoffmann, M.; Kleine-Weber, H.; Schroeder, S.; Kruger, N.; Herrler, T.; Erichsen, S.; Schiergens, T. S.; Herrler, G.; Wu, N. H.; Nitsche, A.; Muller, M. A.; Drosten, C.; Pohlmann, S. SARS-CoV-2 cell entry depends on ACE2 and TMPRSS2 and is blocked by a clinically proven protease inhibitor. *Cell* **2020**, *181* (2), 271–280.
- (7) Gordon, D. E.; Jang, G. M.; Bouhaddou, M.; Xu, J.; Obernier, K.; O’Meara, M. J.; Guo, J. Z.; Swaney, D. L.; Tummino, T. A.; Huttenhain, R.; Kaake, R.; Richards, A. L.; Tutuncuoglu, B.; Foussard, H.; Batra, J.; Haas, K.; Modak, M.; Kim, M.; Haas, P.; Polacco, B. J;

Braberg, H.; Fabius, J. M.; Eckhardt, M.; Soucheray, M.; Brewer, M.; Cakir, M.; McGregor, M. J.; Li, Q.; Naing, Z. Z. C.; Zhou, Y.; Peng, S.; Kirby, I. T.; Melnyk, J. E.; Chorba, J. S.; Lou, K.; Dai, S. A.; Shen, W.; Shi, Y.; Zhang, Z.; Barrio-Hernandez, I.; Memon, D.; Hernandez-Armenta, C.; Mathy, C. J. P.; Perica, T.; Pilla, K. B.; Ganesan, S. J.; Saltzberg, D. J.; Ramachandran, R.; Liu, X.; Rosenthal, S. B.; Calviello, L.; Venkataramanan, S.; Lin, Y.; Wankowicz, S. A.; Bohn, M.; Trenker, R.; Young, J. M.; Cavero, D.; Hiatt, J.; Roth, T.; Rathore, U.; Subramanian, A.; Noack, J.; Hubert, M.; Roesch, F.; Vallet, T.; Meyer, B.; White, K. M.; Miorin, L.; Agard, D.; Emerman, M.; Ruggero, D.; Garc; Amp; iacute-Sastre, A.; Jura, N.; von Zastrow, M.; Taunton, J.; Schwartz, O.; Vignuzzi, M.; d’Enfert, C.; Mukherjee, S.; Jacobson, M.; Malik, H. S.; Fujimori, D. G.; Ideker, T.; Craik, C. S.; Floor, S.; Fraser, J. S.; Gross, J.; Sali, A.; Kortemme, T.; Beltrao, P.; Shokat, K.; Shoichet, B. K.; Krogan, N. J. A SARS-CoV-2 protein interaction map reveals targets for drug repurposing. *Nature* **2020**, *583* (7816), 459–468.

(8) Cheng, F.; Murray, J. L.; Zhao, J.; Sheng, J.; Zhao, Z.; Rubin, D. H. Systems biology-based investigation of cellular antiviral drug targets identified by gene-trap insertional mutagenesis. *PLoS Comput. Biol.* **2016**, *12* (9), No. e1005074.

(9) Zhou, Y.; Hou, Y.; Shen, J.; Huang, Y.; Martin, W.; Cheng, F. Network-based drug repurposing for novel coronavirus 2019-nCoV/SARS-CoV-2. *Cell Discov* **2020**, *6*, 14.

(10) Cheng, F.; Desai, R. J.; Handy, D. E.; Wang, R.; Schneeweiss, S.; Barabasi, A. L.; Loscalzo, J. Network-based approach to prediction and population-based validation of in silico drug repurposing. *Nat. Commun.* **2018**, *9* (1), 2691.

(11) Cheng, F.; Kovacs, I. A.; Barabasi, A. L. Network-based prediction of drug combinations. *Nat. Commun.* **2019**, *10* (1), 1197.

(12) Cheng, F.; Lu, W.; Liu, C.; Fang, J.; Hou, Y.; Handy, D. E.; Wang, R.; Zhao, Y.; Yang, Y.; Huang, J.; Hill, D. E.; Vidal, M.; Eng, C.; Loscalzo, J. A genome-wide positioning systems network algorithm for in silico drug repurposing. *Nat. Commun.* **2019**, *10* (1), 3476.

(13) Stokes, J. M.; Yang, K.; Swanson, K.; Jin, W.; Cubillos-Ruiz, A.; Donghia, N. M.; MacNair, C. R.; French, S.; Carfrae, L. A.; Bloom-Ackerman, Z. J. C.; et al. A deep learning approach to antibiotic discovery. *Cell* **2020**, *180* (4), 688–702.

(14) Zeng, X.; Zhu, S.; Liu, X.; Zhou, Y.; Nussinov, R.; Cheng, F. deepDR: a network-based deep learning approach to in silico drug repositioning. *Bioinformatics* **2019**, *35* (24), S191–S198.

(15) Zheng, S.; Li, Y.; Chen, S.; Xu, J.; Yang, Y. Predicting drug–protein interaction using quasi-visual question answering system. *Nat. Mach. Intell.* **2020**, *2* (2), 134–140.

(16) Zeng, X.; Zhu, S.; Lu, W.; Liu, Z.; Huang, J.; Zhou, Y.; Fang, J.; Huang, Y.; Guo, H.; Li, L. J. C. S.; et al. Target identification among known drugs by deep learning from heterogeneous networks. *Chem. Sci.* **2020**, *11*, 1775–1797.

(17) Wang, M.; Yu, L.; Zheng, D.; Gan, Q.; Gai, Y.; Ye, Z.; Li, M.; Zhou, J.; Huang, Q.; Ma, C.; Huang, Z.; Guo, Q.; Zhang, H.; Lin, H.; Zhao, J.; Li, J.; Smola, A.; Zhang, Z. Deep Graph Library: Towards Efficient and Scalable Deep Learning on Graphs. 2019, arXiv:1909.01315 [cs.LG]. arXiv.org e-Print archive. <https://arxiv.org/pdf/1909.01315.pdf> (accessed March 1, 2020).

(18) Percha, B.; Altman, R. B. J. B. A global network of biomedical relationships derived from text. *Bioinformatics* **2018**, *34* (15), 2614–2624.

(19) Wishart, D. S.; Feunang, Y. D.; Guo, A. C.; Lo, E. J.; Marcu, A.; Grant, J. R.; Sajed, T.; Johnson, D.; Li, C.; Sayeeda, Z. J. N. a. r.; et al. DrugBank 5.0: a major update to the DrugBank database for 2018. *Nucleic Acids Res.* **2018**, *46* (D1), D1074–D1082.

(20) Sun, Z.; Deng, Z.-H.; Nie, J.-Y.; Tang, J. ROTate: Knowledge Graph Embedding by Relational Rotation in Complex Space. 2019, arXiv:1902.10197 [cs.LG]. arXiv.org e-Print archive. <https://arxiv.org/pdf/1902.10197.pdf> (accessed March 1, 2020).

(21) Reghunathan, R.; Jayapal, M.; Hsu, L.-Y.; Chng, H.-H.; Tai, D.; Leung, B. P.; Melendez, A. J. Expression profile of immune response

genes in patients with Severe Acute Respiratory Syndrome. *BMC Immunol.* **2005**, *6* (1), 2.

(22) Jossset, L.; Menachery, V. D.; Gralinski, L. E.; Agnihothram, S.; Sova, P.; Carter, V. S.; Yount, B. L.; Graham, R. L.; Baric, R. S.; Katze, M. G. Cell host response to infection with novel human coronavirus EMC predicts potential antivirals and important differences with SARS coronavirus. *mBio* **2013**, *4* (3), e00165–13.

(23) Yuan, S.; Chu, H.; Chan, J. F.-W.; Ye, Z.-W.; Wen, L.; Yan, B.; Lai, P.-M.; Tee, K.-M.; Huang, J.; Chen, D.; Li, C.; Zhao, X.; Yang, D.; Chiu, M. C.; Yip, C.; Poon, V. K.-M.; Chan, C. C.-S.; Sze, K.-H.; Zhou, J.; Chan, I. H.-Y.; Kok, K.-H.; To, K. K.-W.; Kao, R. Y.-T.; Lau, J. Y.-N.; Jin, D.-Y.; Perlman, S.; Yuen, K.-Y. SREBP-dependent lipidomic reprogramming as a broad-spectrum antiviral target. *Nat. Commun.* **2019**, *10* (1), 120.

(24) Bojkova, D.; Klann, K.; Koch, B.; Widera, M.; Krause, D.; Ciesek, S.; Cinatl, J.; Munch, C. Proteomics of SARS-CoV-2-infected host cells reveals therapy targets. *Nature* **2020**, *583*, 469.

(25) Lamb, J.; Crawford, E. D.; Peck, D.; Modell, J. W.; Blat, I. C.; Wrobel, M. J.; Lerner, J.; Brunet, J. P.; Subramanian, A.; Ross, K. N.; Reich, M.; Hieronymus, H.; Wei, G.; Armstrong, S. A.; Haggarty, S. J.; Clemons, P. A.; Wei, R.; Carr, S. A.; Lander, E. S.; Golub, T. R. The Connectivity Map: using gene-expression signatures to connect small molecules, genes, and disease. *Science* **2006**, *313* (5795), 1929–35.

(26) Sirota, M.; Dudley, J. T.; Kim, J.; Chiang, A. P.; Morgan, A. A.; Sweet-Cordero, A.; Sage, J.; Butte, A. J. Discovery and preclinical validation of drug indications using compendia of public gene expression data. *Sci. Transl. Med.* **2011**, *3* (96), 96ra77.

(27) Powers, D. M. Evaluation: from precision, recall and F-measure to ROC, informedness, markedness and correlation. *J. Mach. Learn. Technol.* **2011**, *2* (1), 37–63.

(28) van der Maaten, L.; Hinton, G. Visualizing data using t-SNE. *J. Mach. Learn. Res.* **2008**, *9*, 2579–2605.

(29) U.S. FDA. Coronavirus (COVID-19) Update: FDA Revokes Emergency Use Authorization for Chloroquine and Hydroxychloroquine. <https://www.fda.gov/news-events/press-announcements/coronavirus-covid-19-update-fda-revokes-emergency-use-authorization-chloroquine-and> (accessed June 20, 2020).

(30) NIH. NIH Halts Clinical Trial of Hydroxychloroquine. <https://www.nih.gov/news-events/news-releases/nih-halts-clinical-trial-hydroxychloroquine> (accessed June 20, 2020).

(31) Chen, G.; Wu, D.; Guo, W.; Cao, Y.; Huang, D.; Wang, H.; Wang, T.; Zhang, X.; Chen, H.; Yu, H.; Zhang, X.; Zhang, M.; Wu, S.; Song, J.; Chen, T.; Han, M.; Li, S.; Luo, X.; Zhao, J.; Ning, Q. Clinical and immunologic features in severe and moderate Coronavirus Disease 2019. *J. Clin. Invest.* **2020**, *130* (5), 2620–2629.

(32) Wang, X.; Xu, W.; Hu, G.; Xia, S.; Sun, Z.; Liu, Z.; Xie, Y.; Zhang, R.; Jiang, S.; Lu, L. SARS-CoV-2 infects T lymphocytes through its spike protein-mediated membrane fusion. *Cell. Mol. Immunol.* **2020**, DOI: 10.1038/s41423-020-0424-9.

(33) Amici, C.; Di Caro, A.; Ciucci, A.; Chiappa, L.; Castilletti, C.; Martella, V.; Decaro, N.; Buonavoglia, C.; Capobianchi, M. R.; Santoro, M. G. Indomethacin has a potent antiviral activity against SARS coronavirus. *Antivir. Ther.* **2006**, *11* (8), 1021–30.

(34) Xu, T.; Gao, X.; Wu, Z.; Selinger, W.; Zhou, Z. Indomethacin has a potent antiviral activity against SARS CoV-2 in vitro and canine coronavirus in vivo. *bioRxiv* **2020**, DOI: 10.1101/2020.04.01.017624.

(35) Castillo, R. R.; Quizon, G. R. A.; Juco, M. J. M.; Roman, A. D. E.; De Leon, D. G.; Punzalan, F. E. R.; Guingon, R. B. L.; Morales, D. D.; Tan, D.-X.; Reiter, R. J. Melatonin as adjuvant treatment for coronavirus disease 2019 pneumonia patients requiring hospitalization (MAC-19 PRO): a case series. *Melatonin Res.* **2020**, *3* (3), 297–310.

(36) Boga, J. A.; Coto-Montes, A.; Rosales-Corral, S. A.; Tan, D. X.; Reiter, R. J. Beneficial actions of melatonin in the management of viral infections: a new use for this “molecular handyman”? *Rev. Med. Virol.* **2012**, *22* (5), 323–38.

(37) Wang, D.; Hu, B.; Hu, C.; Zhu, F.; Liu, X.; Zhang, J.; Wang, B.; Xiang, H.; Cheng, Z.; Xiong, Y.; Zhao, Y.; Li, Y.; Wang, X.; Peng, Z. Clinical characteristics of 138 hospitalized patients with 2019 novel

coronavirus–infected pneumonia in Wuhan, China. *JAMA* **2020**, *323* (11), 1061–1069.

(38) Ramamoorthy, S.; Cidlowski, J. A. Corticosteroids: Mechanisms of action in health and disease. *Rheum. Dis. Clin. North. Am.* **2016**, *42* (1), 15–31.

(39) Li, H.; Chen, C.; Hu, F.; Wang, J.; Zhao, Q.; Gale, R. P.; Liang, Y. Impact of corticosteroid therapy on outcomes of persons with SARS-CoV-2, SARS-CoV, or MERS-CoV infection: a systematic review and meta-analysis. *Leukemia* **2020**, *34* (6), 1503–1511.

(40) Horby, P.; Lim, W. S.; Emberson, J.; Mafham, M.; Bell, J.; Linsell, L.; Staplin, N.; Brightling, C.; Ustianowski, A.; Elmahi, E.; et al. Dexamethasone in hospitalized patients with Covid-19 - Preliminary report. *N. Engl. J. Med.* **2020**, DOI: 10.1056/NEJMoa2021436, (in press).

(41) Lasso, G.; Mayer, S. V.; Winkelmann, E. R.; Chu, T.; Elliot, O.; Patino-Galindo, J. A.; Park, K.; Rabadan, R.; Honig, B.; Shapira, S. D. A structure-informed atlas of human-virus interactions. *Cell* **2019**, *178* (6), 1526–1541.e16.

(42) Zhao, Y.; Ren, J.; Harlos, K.; Jones, D. M.; Zeltina, A.; Bowden, T. A.; Padilla-Parra, S.; Fry, E. E.; Stuart, D. I. Toremifene interacts with and destabilizes the Ebola virus glycoprotein. *Nature* **2016**, *535* (7610), 169–172.

(43) Johansen, L. M.; Brannan, J. M.; Delos, S. E.; Shoemaker, C. J.; Stossel, A.; Lear, C.; Hoffstrom, B. G.; Dewald, L. E.; Schornberg, K. L.; Scully, C.; Lehar, J.; Hensley, L. E.; White, J. M.; Olinger, G. G. FDA-approved selective estrogen receptor modulators inhibit Ebola virus infection. *Sci. Transl. Med.* **2013**, *5* (190), 190ra79.

(44) Cong, Y.; Hart, B. J.; Gross, R.; Zhou, H.; Frieman, M.; Bollinger, L.; Wada, J.; Hensley, L. E.; Jahrling, P. B.; Dyall, J.; Holbrook, M. R. MERS-CoV pathogenesis and antiviral efficacy of licensed drugs in human monocyte-derived antigen-presenting cells. *PLoS One* **2018**, *13* (3), No. e0194868.

(45) Dyall, J.; Coleman, C. M.; Hart, B. J.; Venkataraman, T.; Holbrook, M. R.; Kindrachuk, J.; Johnson, R. F.; Olinger, G. G., Jr.; Jahrling, P. B.; Laidlaw, M.; Johansen, L. M.; Lear-Rooney, C. M.; Glass, P. J.; Hensley, L. E.; Frieman, M. B. Repurposing of clinically developed drugs for treatment of Middle East respiratory syndrome coronavirus infection. *Antimicrob. Agents Chemother.* **2014**, *58* (8), 4885–93.

(46) Kim, Y. I.; Kim, S. G.; Kim, S. M.; Kim, E. H.; Park, S. J.; Yu, K. M.; Chang, J. H.; Kim, E. J.; Lee, S.; Casel, M. A. B.; Um, J.; Song, M. S.; Jeong, H. W.; Lai, V. D.; Kim, Y.; Chin, B. S.; Park, J. S.; Chung, K. H.; Foo, S. S.; Poo, H.; Mo, I. P.; Lee, O. J.; Webby, R. J.; Jung, J. U.; Choi, Y. K. Infection and rapid transmission of SARS-CoV-2 in ferrets. *Cell Host Microbe* **2020**, *27* (5), 704–709.

(47) Valavaara, R.; Pyrhonen, S.; Heikkinen, M.; Rissanen, P.; Blanco, G.; Tholix, E.; Nordman, E.; Taskinen, P.; Holsti, L.; Hajba, A. Toremifene, a new antiestrogenic compound, for treatment of advanced breast cancer. Phase II study. *Eur. J. Cancer Clin. Oncol.* **1988**, *24* (4), 785–90.

(48) Thompson, I. M., Jr.; Leach, R. Prostate cancer and prostatic intraepithelial neoplasia: true, true, and unrelated? *J. Clin. Oncol.* **2013**, *31* (5), 515–6.

(49) Kivinen, S.; Maenpaa, J. Effect of toremifene on clinical chemistry, hematology and hormone levels at different doses in healthy postmenopausal volunteers: phase I study. *J. Steroid Biochem.* **1990**, *36* (3), 217–220.

(50) Liu, J.; Cao, R.; Xu, M.; Wang, X.; Zhang, H.; Hu, H.; Li, Y.; Hu, Z.; Zhong, W.; Wang, M. Hydroxychloroquine, a less toxic derivative of chloroquine, is effective in inhibiting SARS-CoV-2 infection in vitro. *Cell Discovery* **2020**, *6*, 16.

(51) Chen, Z.; Hu, J.; Zhang, Z.; Jiang, S.; Han, S.; Yan, D.; Zhuang, R.; Hu, B.; Zhang, Z. Efficacy of hydroxychloroquine in patients with COVID-19: results of a randomized clinical trial. *medRxiv* **2020**, DOI: 10.1101/2020.03.22.20040758.

(52) Chorin, E.; Dai, M.; Shulman, E.; Wadhvani, L.; Bar Cohen, R.; Barbhayya, C.; Aizer, A.; Holmes, D.; Bernstein, S.; Soinelli, M.; Park, D. S.; Chinitz, L.; Jankelsohn, L. The QT interval in patients with

SARS-CoV-2 infection treated with hydroxychloroquine/azithromycin. *medRxiv* **2020**, DOI: [10.1101/2020.04.02.20047050](https://doi.org/10.1101/2020.04.02.20047050).

(53) Rajeshkumar, N. V.; Yabuuchi, S.; Pai, S. G.; Maitra, A.; Hidalgo, M.; Dang, C. V. Fatal toxicity of chloroquine or hydroxychloroquine with metformin in mice. *bioRxiv* **2020**, DOI: [10.1101/2020.03.31.018556](https://doi.org/10.1101/2020.03.31.018556).

(54) Gassen, N. C.; Niemeyer, D.; Muth, D.; Corman, V. M.; Martinelli, S.; Gassen, A.; Hafner, K.; Papies, J.; Mosbauer, K.; Zellner, A.; Zannas, A. S.; Herrmann, A.; Holsboer, F.; Brack-Werner, R.; Boshart, M.; Muller-Myhsok, B.; Drosten, C.; Muller, M. A.; Rein, T. SKP2 attenuates autophagy through Beclin1-ubiquitination and its inhibition reduces MERS-Coronavirus infection. *Nat. Commun.* **2019**, *10* (1), 5770.

(55) Shi, J.; Wen, Z.; Zhong, G.; Yang, H.; Wang, C.; Huang, B.; Liu, R.; He, X.; Shuai, L.; Sun, Z.; Zhao, Y.; Liu, P.; Liang, L.; Cui, P.; Wang, J.; Zhang, X.; Guan, Y.; Tan, W.; Wu, G.; Chen, H.; Bu, Z. Susceptibility of ferrets, cats, dogs, and other domesticated animals to SARS-coronavirus 2. *Science* **2020**, *368* (6494), 1016–1020.